NANO LETTERS

2009
Vol. 9, No. 7
2704-2709

Electric Field Control of Magnetoresistance in InP Nanowires with Ferromagnetic Contacts

F. A. Zwanenburg, D. W. van der Mast, H. B. Heersche, and L. P. Kouwenhoven*

Kavli Institute of Nanoscience, Delft University of Technology, P.O. Box 5046, 2600 GA Delft, The Netherlands

E. P. A. M. Bakkers

Philips Research Laboratories, Professor Holstlaan 4, 5656 AA Eindhoven, The Netherlands

Received April 14, 2009; Revised Manuscript Received June 2, 2009

Downloaded by UKB CONSORTIA NETHERLANDS on July 8, 2009
Published on June 18, 2009 on http://pubs.acs.org | doi: 10.1021/nl901184m

ABSTRACT

We demonstrate electric field control of sign and magnitude of the magnetoresistance in InP nanowires with ferromagnetic contacts. The sign change in the magnetoresistance is directly correlated with a sign change in the transconductance. Additionally, the magnetoresistance is shown to persist at such a high bias that Coulomb blockade has been lifted. We also observe the magnetoresistance when one of the ferromagnets is replaced by a nonmagnetic metal. We conclude that it must be induced by a single ferromagnetic contact, and that spin transport can be ruled out as the origin. Our results emphasize the importance of a systematic investigation of spin-valve devices in order to discriminate between ambiguous interpretations.

1. Introduction. The realization of the field effect transistor in 1947 may be the greatest invention of the 20th century, allowing the development of modern-day electronics. The discovery of the giant magnetoresistance in multilayers of magnetic and nonmagnetic metals[1,2] has had an enormous impact on the data storage industry. It opened the field of spintronics that wants to exploit both the spin and charge degree of freedom of electrons for useful devices.[3−5] The proposal of Datta and Das, that combines the functionalities of semiconductors and magnetic materials into a spin transistor,[6] has triggered many research groups to pursue its experimental realization.

The typical signature of giant magnetoresistance, or spin valve effect, is the onset of a low and high resistance state for parallel (P) and antiparallel (AP) orientations of the magnetizations of two ferromagnets. These different magnetization directions result in different densities of states for spin-up and spin-down electrons at the Fermi energy. Using this imbalance, one can inject a majority of electrons with either spin-up or spin-down into a nonmagnetic material. In metallic systems spin transport is a well-understood phenomenon, but it took almost a decade until the first demonstration was claimed on carbon nanotubes with ferromagnetic contacts,[7] after which many followed.[8−14]

However, the Magneto-Coulomb effect can have the exact same signature, resulting in ambiguous interpretations of spin transport experiments.[15] Magneto-Coulomb oscillations were first observed in ferromagnetic single electron transistors in 1997.[16,17] These experiments showed how a magnetic field can induce single electron charging effects: a change in magnetic field B shifts the densities of states for spin-up and spin-down electrons in a ferromagnet by the Zeeman energy $\Delta E_Z = \pm g\mu_B B/2$. Here g is the gyromagnetic ratio, μ_B is the Bohr magneton, and the sign is negative (positive) for spin-up (spin-down). The total number of electrons stays constant, and as a consequence the chemical potential has to change by $P\Delta E_Z$ with P as the spin polarization at the Fermi energy. If the ferromagnet is capacitively coupled to the metallic island of a single electron transistor, the resulting modification in work function acts as a voltage on a gate. Via this mechanism a magnetic field can give rise to single electron charging effects. Along these lines the Magneto-Coulomb effect should also be observable in semiconductors contacted by ferromagnets.

Here we present the first experiments on semiconductor nanowires with ferromagnetic contacts. We use InP nanowires that are contacted with both ferromagnetic and nonmagnetic metals, allowing for discrimination of spin transport effects and the Magneto-Coulomb effect, thus avoiding ambiguous interpretations of the experiments. We demon-

* To whom correspondence should be addressed. E-mail: l.p.kouwenhoven@tudelft.nl.

10.1021/nl901184m CCC: $40.75 © 2009 American Chemical Society
Published on Web 06/18/2009

strate electric field control of the sign and magnitude of the magnetoresistance in these devices. Additionally, the magnetoresistance is shown to persist at a high bias where the quantum dot regime is no longer relevant.

If one wants to inject and detect spins electrically, the nonlocal measurement of a spin imbalance[18,19] is generally regarded as the best configuration to exclude misleading effects that leave the same signature. Only recently three nonlocal experiments have been reported in nonmetallic systems, namely carbon nanotubes,[20] GaAs,[21] and graphene.[22] In our devices, we measure a magnetic hysteresis with only one visible switch (not shown here). We have measured the nonlocal voltage in more than 20 different samples at different current biases and gate voltages, but we never observe a spin-valve like signal. The results on carbon nanotubes with ferromagnetic contacts[8−14] were all carried out in a 2-point (or "local") geometry. They observed the typical spin valve-like signal of a low- and high resistance state for parallel and antiparallel orientations of the magnetizations of the ferromagnetic electrodes, which does not allow an unambiguous interpretation.

Crystalline InP nanowires are grown from gold catalyst particles via a vapor−liquid−solid process[23−25] by using laser ablation. During growth Se is incorporated as dopant atom (100 ppm Se). The effective doping level corresponds to $\sim 10^{19}$ cm^{-3}. The typical diameter is 50 nm and lengths vary from 5 to 20 μm. After growth, we deposit the nanowires on a thermally oxidized silicon wafer with 250 nm SiO_2. The silicon is highly doped, enabling use of it as a backgate to induce an electric field in the nanowires. Predeposited markers allow locating individual nanowires and definition of electrodes by means of electron-beam lithography. Before metal deposition, the samples are treated with buffered hydrofluoric acid for 5 s in order to etch off the native oxide layer around the nanowires. We then evaporate 100 nm of the alloy $Co_{80}Fe_{20}$ for ferromagnetic contacts. After a second lithography step and etch treatment, 110 nm Ti/Pt is deposited for nonmagnetic contacts. In the experiments shown here, the distance between the contacts is varied from 200 to 460 nm. The resulting two-point resistances are typically 20−80 kΩ but can be as low as 5 kΩ. For both CoFe-InP and Ti/Pt-InP, the contact resistance is estimated between 1 and 10 kΩ. The high carrier concentration results in a very thin Schottky barrier. At low temperature, we see an increase in differential resistance around zero bias, but no sign of Coulomb blockade. Measurements of the conductance versus source-drain and backgate voltage show an interference pattern that most likely originates from universal conductance fluctuations or Fabry−Pérot-like interference between source and drain contacts. The presented data in this paper are taken at 1.6−1.8 K in a pumped ^{4}He-cryostat. We only show two-terminal measurements, where we bias a DC current from source to drain and measure the source−drain voltage.

2. Electric Field Control of Magnetoresistance. Figure 1A shows a scanning electron micrograph of device A, an InP nanowire with four CoFe (F) contacts. Two contacts have a width of 100 nm and the other two 300 nm, resulting in different coercive fields. When the magnetic field is swept parallel to the easy axis of the contacts, the magnetizations of the wider (300 nm) electrodes will switch before the two 100 nm electrodes. This allows us to measure the device resistance both with parallel and antiparallel magnetizations of the involved electrodes. The distance between the contacts is about 200 nm, and the device has a resistance of 10 kΩ at zero gate voltage. The devices B and C (later in this paper) have almost identical designs and differential resistances of 15−20 and 140−260 kΩ, respectively.

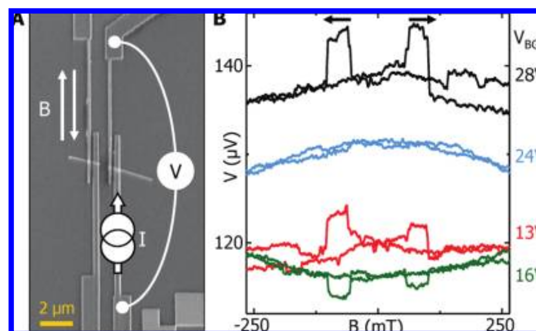

Figure 1. Electric field control of magnetoresistance. (A) SEM of device A, an InP nanowire with four CoFe contacts. The electrodes have different widths (100 and 300 nm) in order to realize different coercive fields. We perform two-terminal measurements on the two rightmost contacts, which are separated by 220 nm. The wire part between the middle contacts has broken off after metal lift-off and is not used for measurements. We bias a DC current I from source to drain and measure the source−drain voltage V. The other contacts are floating. (B) Magnetic field sweeps at 2 K of the voltage at a current bias of 10 nA for different values of the backgate voltage. The magnetic field is swept up and down parallel to the easy axis of the electrodes; arrows indicate the sweep direction. At three of the four backgate voltages, the magnetization switches at ±55 and ±100 mT result in jumps in the measured voltage varying from −1.4 to +2.3%.

The magnetization switches are clearly visible in the measured voltage at a constant current bias of 10 nA; see Figure 1B. When the magnetic field is swept in the positive direction, jumps in the voltage appear at 55 and 100 mT. Going to negative fields two jumps are seen symmetrically in B-field. Between ±55 mT and ±100mT the two ferromagnets have antiparallel magnetizations. Outside these regions they are aligned parallel, either in the positive or negative B-field direction. Four sets of traces are shown at backgate voltages of 13, 16, 24, and 28 V. When we define the magnetoresistance as $(R_{AP} - R_P/(R_{AP} + R_P)$ we find respective values of 1.4, −1.0, 0, and 2.3% for these gate voltages. Besides observing the two-terminal magnetoresistance in more than 20 different F-InP-F devices, we have also measured the magnetoresistance of a nanowire in a four-point geometry; we measured the voltage between the inner two contacts of a nanowire with a constant bias current through the outer two electrodes (all ferromagnetic). This resulted in the same magnetoresistance as in a two-point measurement on the inner two contacts, both qualitatively and quantitatively. The results in Figure 1 demonstrate that we can control and even turn off the magnetoresistance by means of an electric field.

Downloaded by UKB CONSORTIA NETHERLANDS on July 8, 2009
Published on June 18, 2009 on http://pubs.acs.org | doi: 10.1021/nl901184m

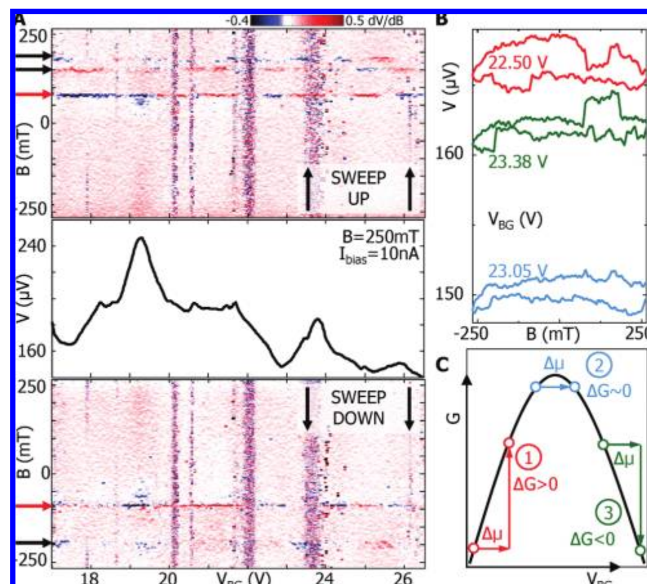

Figure 2. Relationship between transconductance and magnetoresistance. (A) For device B, the voltage is measured at a current bias of 10 nA. The colorscale plots show the numerical derivative dV/dB versus magnetic field and gate voltage. The upper (lower) panel depicts the magnetoresistance while sweeping the magnetic field up (down). Red (blue) represents a positive (negative) magnetoresistance. Three switches are visible at ±80, +150, and ±190 mT. The first can be attributed to the 300 nm wide CoFe electrode, and the latter two to the 100 nm contact (its magnetization switches in two steps). The middle panel shows a line cut of the measured voltage versus gate voltage at $B = 250$ mT, taken from the upper panel. (B) Line cuts of panel A at three different gate voltages. The magnetoresistance changes sign while the normal resistance goes through a minimum at $V_{BG} = 22.9$ V. (C) Schematic explaining sign change of the conductance in case of the Magneto-Coulomb effect. If the chemical potential μ of one of the ferromagnetic contacts changes by an amount $\Delta\mu$, it results in an effective ΔV_{BG} on the device. The change in conductance G depends on the position in gate space. When the conductance goes through a maximum it can change from $\Delta G > 0$ (before the maximum, situation 1) to $\Delta G = 0$ (situation 2) to $\Delta G < 0$ (situation 3).

Downloaded by UKB CONSORTIA NETHERLANDS on July 8, 2009
Published on June 18, 2009 on http://pubs.acs.org | doi: 10.1021/nl901184m

3. Relationship between Transconductance and Magnetoresistance. Now we look in more detail at the relation between the sign of the magnetoresistance and the transconductance. With no gate voltage applied, device B has a differential resistance of 18 kΩ at zero bias and 15 kΩ at a bias of 100 nA. We perform the same magnetic field sweeps as on device A while stepping the gate voltage from 17 to 26.5 V. It turns out that the change in resistance with electric field (∼20%) is much bigger than the sudden change due to the switches (∼0.5−1% in this device). Plotting the numerical derivative dV/dB, which is proportional to the magnetoresistance, allows us to discern the magnetization switches.

Figure 2A shows a colorscale plot of dV/dB versus backgate voltage and magnetic field. The switches appear as horizontal alternating red and blue lines at ±80, +150, and ±190 mT. In the measurement setup, the magnetic field was not aligned with the easy axis but under a nonzero angle with the electrodes. This results in higher switching fields for both CoFe contacts, and one of the electrodes switches in two parts (at 150 and 190 mT). The switching lines change from red to blue or vice versa a couple of times, corresponding to a sign change in magnetoresistance. There are several minima and maxima in the device resistance versus backgate voltage; see middle panel in Figure 2A. The three line cuts in Figure 2B are taken around the minimum at $V_{BG} = 22.9$ V. The sign of the magnetoresistance changes from negative at $V_{BG} = 22.5$ V to zero (at $V_{BG} = 23.05$ V) to positive (at $V_{BG} = 23.38$ V). We have observed this in devices A and C as well. These results show that a sign change in the transconductance, dG/dV_{BG}, goes together with a sign change in the magnetoresistance.

4. Magneto-Coulomb Effect and Spin Transport. The origin of this relationship can be understood by both the Magneto-Coulomb effect and spin transport.

The experiments on carbon nanotubes with ferromagnetic contacts[8–14] are in the coulomb blockade regime, and the presented magnetic field sweeps display the spin-valve signature. Different mechanisms are suggested to explain the data, namely spin injection, spin-dependent quantum interference, and spin-dependent coupling between quantum dot and lead. The latter two[12,13] reported the correlation of sign changes of their magnetoconductance with resonances in the normal conductance, just like in Figure 2A,B. Man et al. add the disappearance of the effect on increasing the voltage bias of the device.[13]

The Magneto-Coulomb effect has been demonstrated and carefully explained for the first time in metallic devices by Ono et al.[17] In this case, a change in magnetic field shifts the densities of states for spin-up and spin-down electrons in a ferromagnet by the Zeeman energy $\Delta E_Z = \pm g\mu_B B/2$. Since the spin-up and spin-down densities of states differ and the total number of electrons stays constant, the chemical potential has to change by

$$\Delta\mu = \pm P g\mu_B B/2 \tag{1}$$

Here P is the spin polarization of the electron density of states at the Fermi energy of the ferromagnet. The work function of the ferromagnet changes by the same amount as μ. When the ferromagnet is capacitively coupled to an island via a capacitance C, the charge on the island changes by $\Delta q = C\Delta\mu/e$.[15] Adding up all contributions leads to the total accumulated charge

$$\Delta q = C_S\Delta V_S + C_D\Delta V_D + C_{BG}\Delta V_{BG} \tag{2}$$

where the subscripts S, D, and BG refer to source, drain, and backgate.

Equations 1 and 2 demonstrate how an applied magnetic field can change the electric field experienced by the device (Figure 2C). The corresponding change in the conductance depends on the transconductance. When the conductance goes over a peak, it can change from $\Delta G > 0$ (before the peak, situation 1) to $\Delta G = 0$ (situation 2) to $\Delta G < 0$ (situation 3). This is an adequate explanation for the magnetoresistance at different gate voltages as shown in Figure 1 and 2.

We stress that in order for the latter effect to be observed only one ferromagnetic contact is sufficient. In contrast,

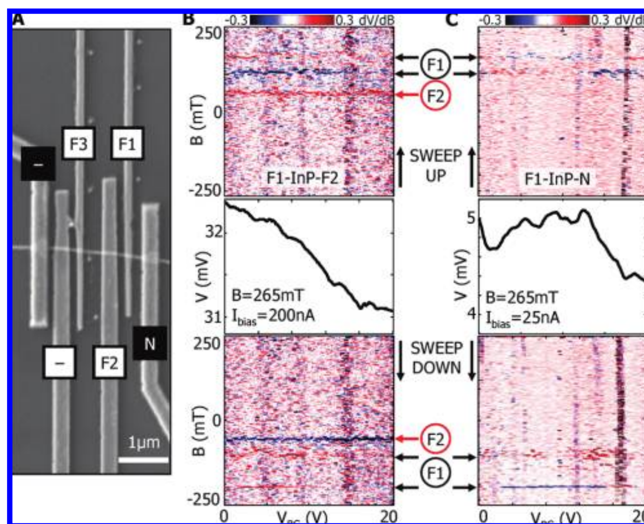

Figure 3. Magnetic field sweeps on device C: an InP wire with four ferromagnetic and two normal contacts. (A) SEM of the device. The two leftmost electrodes are not connected. (B) F1-InP-F2: we measure V from F1 to F2 in the range $V_{BG} = [0,20\ V]$ at a current bias of 200 nA while sweeping the magnetic field up (top panel) and down (bottom panel). The jumps caused by the magnetization switches are highlighted in blue and red. In both sweep directions three magnetization switches are visible at ±60, ±110, and +170/−200 mT. The first switch can be attributed to F2, and latter two to F1. (C) F1-InP-N: we measure V from F1 to N at a current bias of 25 nA. The switch of F2 at ±60 mT has disappeared. However, the two switches at ±110 and +170/−200 mT are still visible. Both are caused by the magnetization switching of F1, which means that the observed magnetoresistance is induced by one ferromagnetic contact alone.

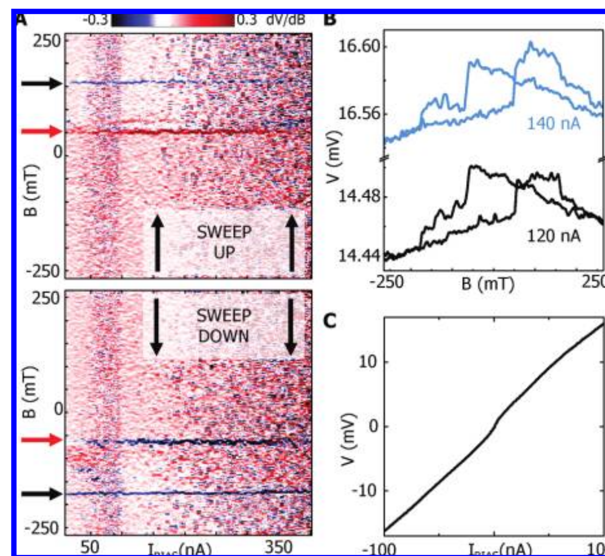

Figure 4. Bias dependence of the magnetoresistance of device C. (A) The upper (lower) panel shows dV/dB in colorscale versus current bias while the magnetic field is swept up (down). This is the same device as in Figure 3, but here we use F2 and F3. The gate voltage is kept at $V_{BG} = 0$ V. The sign and magnitude of the magnetoresistance do not change with increasing bias current. (B) Line cuts of panel A at current biases of 120 and 140 nA. The two voltage jumps in the negative sweep direction have the same sign. (C) Current−Voltage characteristic at zero B-field and zero gate voltage. dV/dI varies from 130 kΩ at 100 nA to 260 kΩ at zero bias.

Downloaded by UKB CONSORTIA NETHERLANDS on July 8, 2009
Published on June 18, 2009 on http://pubs.acs.org | doi: 10.1021/nl901184m

electrical detection of spin transport requires spin coherence from one ferromagnet to another, and therefore at least two ferromagnets are necessary for that experiment. Using only one ferromagnetic contact results in two possible scenarios. (i) The signal is absent, indicating spin transport as the origin. (ii) The signal of one magnetization switch is present, proving that the Magneto-Coulomb effect causes the magnetoresistance.

5. Magnetoresistance with One Ferromagnet. To find out which effect comes into play in our experiment we have fabricated devices with both ferromagnetic and normal contacts to InP nanowires. We have performed magnetic field and electric field sweeps on device C, which has three working CoFe contacts and one working Ti/Pt contact, see Figure 3A. The differential resistance of both combinations CoFe-InP-CoFe (F-InP-F) and CoFe-InP-Ti/Pt (F-InP-N) is ∼230 kΩ at zero bias and ∼150 kΩ at a bias of 100 nA. Figure 3B shows the magnetoresistance in colorscale versus gate voltage for the F-InP-F configuration.

Just like in Figure 2 three distinct resistance jumps show up at ±60, ±110, and +170/−200 mT, which we can relate to the coercive fields of F1 (±110 mT and +170 mT/−200) and F2 (±60 mT). Contrary to the measurements of Figures 1 and 2, the magnetoresistance barely changes with respect to gate voltage. The reason is that the gate dependence of the conductance has no minima or maxima; at this current bias, the conductance only goes up with increasing gate voltage, see middle panel of 3B. When we carry out the same measurement in the F-InP-N configuration, we still see the two jumps that correspond to the magnetization switching of F1 (Figure 3C), but the coercive field of F2 at ±60 mT is no longer visible. We observe the same signature at a current bias of 3 nA. Apparently we do not need two ferromagnetic electrodes to observe a resistance jump caused by a magnetization switch. We conclude from Figure 3 that the magnetoresistance is induced by a single ferromagnetic contact.

6. Magnetoresistance at High Bias. We have also investigated whether the magnetoresistance remains at high current bias. Figure 4A shows the magnetic field sweeps on device C while the current bias is swept from 10 to 400 nA. Here we use F2 and the third ferromagnetic contact F3 with an InP channel length of 460 nm. Throughout the entire bias range jumps appear at ±60 and ±170 mT, caused by the magnetization switches of, respectively, F2 and F3. Above 250 nA, the jumps are more difficult to resolve due to instability of the device at high current bias, but they are present nevertheless. The sign and relative magnitude of the magnetoresistance do not change when the bias current is increased up to 400 nA.

In the negative sweep direction of both traces in Figure 4B, two jumps in voltage of about −20 and −10 μV are visible at −60 and −170mT, corresponding to a conductance change of 0.1 and 0.05%. In Figure 4C we plot the IV of F2-InP-F3. The presence of the switches at high bias indicates that single electron charging is not necessary to observe the coercive fields of the ferromagnets. This is confirmed by Figure 3B where the switches appear at a high

bias of 200 nA. In order to be complete we have measured the bias dependence of device B as well, and saw no change in the magnetoresistance when the bias was varied from 1 nA to 225 nA (not shown here). The results in Figure 4 demonstrate that the magnetoresistance persists at a high bias where the quantum dot regime is no longer relevant.

The data in Figures 3 and 4 demonstrate that we are dealing with a ferromagnetic contact-induced effect, visible without the necessity of Coulomb blockade. Figure 3 demonstrates that the observed magnetoresistance is not related to coherent spin transport from one ferromagnet to another. Also, the fact that both voltage jumps in the negative sweep direction can go down (e.g., Figure 4B, down-sweep) means there are more than two resistance levels in a magnetic field sweep. That excludes a direct correlation of low- and high-resistance states of the device as the direct result of P and AP configurations of the ferromagnets.

7. Discussion. On the basis of the results in Figures 3 and 4, spin transport can be eliminated as a plausible explanation of the magnetoresistance; see the Supporting Information for a discussion of the different interpretations. Qualitatively the Magneto-Coulomb effect can account for all our measurements. When we extract the change in chemical potential $\Delta\mu$ from our data we find $\Delta\mu = 165$ meV, whereas eq 1 would yield a theoretical value for $\Delta\mu$ of 5 μeV; see Supporting Information for details. The theoretical prediction is 4 orders of magnitude smaller than the empirical value. This quantitative difference suggests a stronger change in work function than eq 1 predicts, which may be caused by anisotropic density of states in the ferromagnet.

Recently there have been reports of spin−orbit induced tunneling anisotropic magnetoresistance caused by a single Fe[26] and a single Co[27] contact. In ferromagnetic metals anisotropic magnetoresistance stems from spin−orbit interaction, which mixes the conductive s-bands with the exchange-split d-bands. Free particle-like s-states determine the transport properties of a metal. The density of states of the d-bands depends on the direction of the magnetization. Therefore spin−orbit induced scattering of electrons from conductive s-states into localized d-states increases the resistivity of the metal. A magnetization switch thus affects the conductivity by changing the density of states of the d-bands.

Analogously, in tunnel devices with a ferromagnetic contact the density of states can be anisotropic and depend on the direction of the magnetization. The anisotropy can be sensed by electrons tunneling into or from the ferromagnet. In our F-InP junctions, the deposited CoFe electrodes are wrapped around the InP nanowire, resulting in a locally very strong shape anisotropy at the interface. The surface charges of the CoFe contacts add a component to the external magnetic field. This demagnetizing field can be roughly 1 T, which shifts the local work function of the ferromagnet by 50 μeV according to eq 1. Since each contact is different on a microscopic scale, there will be a wide variety in anisotropies of all electrode shapes. The direction of the tunneling current relative to the magnetization direction is unique for each individual interface. The shape anisotropy can thus add a significant contribution to the change in work function, and may accordingly confirm the values we found. A calculation of this contribution is not feasible since the evaporated CoFe is polycrystalline; the dependence of density of states on the magnetization direction is not as straightforward as, for example, for single crystals.[28]

In conclusion, we have reported the first observation of magnetoresistance in semiconductor nanowires with ferromagnetic contacts. The electric field control of sign and magnitude of the magnetoresistance displays a direct correlation with the transconductance. Also, the methods we use allow discrimination between effects induced by the contacts and spin transport phenomena. We observe the magnetoresistance when one of the ferromagnets is replaced by a nonmagnetic metal, ruling out spin transport and proving that it is caused by a single ferromagnetic contact. We attribute the magnetoresistance to the Magneto-Coulomb effect, where a magnetically induced change in its work function alters the electric field experienced by the InP nanowire and hence the total device resistance. Our results emphasize the importance of making the distinction between different effects with the exact same signature to avoid ambiguous interpretations of magnetoresistance measurements.

Acknowledgment. We thank G. E. W. Bauer, A. J. S. Bernand-Mantel, J. A. van Dam, D. Loss, G. A. Steele, and B. J. van Wees for discussions. Supported by the Dutch Organization for Fundamental Research on Matter (FOM), The Netherlands Organization for Scientific Research (NWO) and NanoNed, a national nanotechnology program coordinated by the Dutch Ministry of Economic Affairs.

Supporting Information Available: This material is available free of charge via the Internet at http://pubs.acs.org.

References

(1) Baibich, M. N.; Broto, J. M.; Fert, A.; Van Dau, F. N.; Petroff, F.; Eitenne, P.; Creuzet, G.; Friederich, A.; Chazelas, J. Giant Magnetoresistance of (001) Fe/(001) Cr Magnetic Superlattices. *Phys. Rev. Lett.* **1988**, *61* (21), 2472–2475.
(2) Binasch, G.; Grünberg, P.; Saurenbach, F.; Zinn, W. Enhanced magnetoresistance in layered magnetic structures with antiferromagnetic interlayer exchange. *Phys. Rev. B* **1989**, *39* (7), 4828–4830.
(3) Prinz, G. A. Magnetoelectronics. *Science* **1998**, *282*, 1660–1663.
(4) Wolf, S. A.; et al. A Spintronics: A Spin-Based Electronics Vision for the Future. *Science* **2001**, *294*, 1488−1495.
(5) Zutic, I.; Fabian, J.; Sarma, S. D. Spintronics: Fundamentals and applications. *Rev. Mod. Phys.* **2004**, *76*, 323−410.
(6) Datta, S.; Das, B. Electronic analog of the electro-optic modulator. *Appl. Phys. Lett.* **1990**, *56*, 665.
(7) Tsukagoshi, K.; Alphenaar, B. W.; Ago, H. Coherent transport of electron spin in a ferromagnetically contacted carbon nanotube. *Nature* **1999**, *401*, 572–574.
(8) Orgassa, D.; Mankey, G. J.; Fujiwara, H. Spin injection into carbon nanotubes and a possible application in spin-resolved scanning tunnelling microscopy. *Nanotechnology* **2001**, *12* (3), 281–284.
(9) Zhao, B.; Mönch, I.; Vinzelberg, H.; Mühl, T.; Schneider, C. Spin-coherent transport in ferromagnetically contacted carbon nanotubes. *Appl. Phys. Lett.* **2002**, *80*, 3144.

Downloaded by UKB CONSORTIA NETHERLANDS on July 8, 2009
Published on June 18, 2009 on http://pubs.acs.org | doi: 10.1021/nl901184m

(10) Kim, J. R.; So, H. M.; Kim, J. J.; Kim, J. Spin-dependent transport properties in a single-walled carbon nanotube with mesoscopic Co contacts. *Phys. Rev. B* **2002**, *66* (23), 233401.
(11) Jensen, A.; Hauptmann, J. R.; Nygård, J.; Lindelof, P. E. Magnetoresistance in ferromagnetically contacted single-wall carbon nanotubes. *Phys. Rev. B* **2005**, *72* (3), 35419.
(12) Sahoo, S.; Kontos, T.; Furer, J.; Hoffmann, C.; Gräber, M.; Cottet, A.; Schönenberger, C. Electric field control of spin transport. *Nat. Phys.* **2005**, *1*, 99–102.
(13) Man, H. T.; Wever, I. J. W.; Morpurgo, A. F. Spin-dependent quantum interference in single-wall carbon nanotubes with ferromagnetic contacts. *Phys. Rev. B* **2006**, *73* (24), 241401.
(14) Hueso, L. E.; Pruneda, J. M.; Ferrari, V.; Burnell, G.; Valdés-Herrera, J. P.; Simons, B. D.; Littlewood, P. B.; Artacho, E.; Fert, A.; Mathur, N. D. Transformation of spin information into large electrical signals using carbon nanotubes. *Nature* **2007**, *445*, 410–413.
(15) van der Molen, S. J.; Tombros, N.; van Wees, B. J. Magneto-Coulomb effect in spin-valve devices. *Phys. Rev. B* **2006**, *73*, 220406.
(16) Ono, K.; Shimada, H.; Ootuka, Y. Enhanced Magnetic Valve Effect and Magneto-Coulomb Oscillations in Ferromagnetic Single Electron Transistor. *J. Phys. Soc. Jpn.* **1997**, *66*, 1261.
(17) Shimada, H.; Ono, K.; Ootuka, Y. Magneto-Coulomb Oscillation in Ferromagnetic Single Electron Transistors. *J. Phys. Soc. Jpn.* **1998**, *67*, 1359.
(18) Johnson, M.; Silsbee, R. H. Interfacial charge-spin coupling: Injection and detection of spin magnetization in metals. *Phys. Rev. Lett.* **1985**, *55* (17), 1790–1793.
(19) Jedema, F. J.; Heersche, H. B.; Filip, A. T.; Baselmans, J. J. A.; van Wees, B. J. Electrical detection of spin precession in a metallic mesoscopic spin valve. *Nature* **2002**, *416*, 713–716.
(20) Tombros, N.; van der Molen, S. J.; van Wees, B. J. Separating spin and charge transport in single-wall carbon nanotubes. *Phys. Rev. B* **2006**, *73* (23), 233403.
(21) Lou, X.; Adelmann, C.; Crooker, S. A.; Garlid, E. S.; Zhang, J.; Reddy, S. M.; Flexner, S. D.; Palmstrom, C. J.; Crowell, P. A. Electrical detection of spin transport in lateral ferromagnet--semiconductor devices. *Nat. Phys.* **2007**, *3*, 197–202.
(22) Tombros, N.; Jozsa, C.; Popinciuc, M.; Jonkman, H. T.; van Wees, B. J. Electronic spin transport and spin precession in single graphene layers at room temperature. *Nature* **2007**, *448*, 571–574.
(23) Wagner, R. S.; Ellis, W. C. Vapor-Liquid Mechanism of Single Crystal Growth. *Appl. Phys. Lett.* **1964**, *4*, 89–90.
(24) Bakkers, E. P. A. M.; van Dam, J. A.; De Franceschi, S.; Kouwenhoven, L. P.; Kaiser, M.; Verheijen, M.; Wondergem, H.; van der Sluis, P. Epitaxial growth of InP nanowires on germanium. *Nat. Mater.* **2004**, *3*, 769−773.
(25) De Franceschi, S.; van Dam, J. A.; Bakkers, E. P. A. M.; Feiner, L. F.; Gurevich, L.; Kouwenhoven, L. P. Single-electron tunneling in InP nanowires. *Appl. Phys. Lett.* **2003**, *83*, 2, 344.
(26) Moser, J.; Matos-Abiague, A.; Schuh, D.; Wegscheider, W.; Fabian, J.; Weiss, D. Tunneling Anisotropic Magnetoresistance and Spin-Orbit Coupling in Fe/GaAs/Au Tunnel Junctions. *Phys. Rev. Lett.* **2007**, *99* (5), 56601.
(27) Liu, R. S.; Michalak, L.; Canali, C. M.; Samuelson, L.; Pettersson, H. Tunneling Anisotropic Magnetoresistance in Co/AlO_x/Au Tunnel Junctions. *Nano Lett* **2008**, *8* (3), 848–852.
(28) Bode, M.; Heinze, S.; Kubetzka, A.; Pietzsch, O.; Nie, X.; Bihlmayer, G.; Blügel, S.; Wiesendanger, R. "Magnetization-Direction-Dependent Local Electronic Structure Probed by Scanning Tunneling Spectroscopy. *Phys. Rev. Lett.* **2002**, *89* (23), 237205. and references in Supplementary Information.

NL901184M

Downloaded by UKB CONSORTIA NETHERLANDS on July 8, 2009
Published on June 18, 2009 on http://pubs.acs.org | doi: 10.1021/nl901184m